K. MIŁKOWSKA-PISZCZEK*, M. RYWOTYCKI*, J. FALKUS*, K. KONOPKA

A COMPARISON OF MODELS DESCRIBING HEAT TRANSFER IN THE PRIMARY COOLING ZONE OF A CONTINUOUS CASTING MACHINE

PORÓWNANIE MODELI OPISUJĄCYCH WYMIANĘ CIEPŁA W PIERWOTNEJ STREFIE CHŁODZENIA MASZYNY COS

This paper presents the findings of research conducted concerning the determination of thermal boundary conditions for the steel continuous casting process within the primary cooling zone. A cast slab - with dimensions of 1100 mm×220 mm – was analysed, and models described in references were compared with the authors' model. The presented models were verified on the basis of an industrial database. The research problem was solved with the finite element method using the ProCAST software package.

Keywords: continuous casting of steel, heat transfer coefficient, numerical modelling, ProCAST

W pracy przedstawiono wyniki badań dotyczących wyznaczenia termicznych warunków brzegowych dla procesu ciągłego odlewania stali w obszarze strefy pierwotnego chłodzenia. Analizie poddano wlewek płaski o wymiarach 1100×220 mm. W obliczeniach porównano modele opisane w literaturze wraz z modelem własnym. Zaprezentowane modele zweryfikowano na podstawie przemysłowej bazy danych. Zadanie zostało rozwiązane metodą elementów skończonych z zastosowaniem pakietu oprogramowania ProCAST.

1. Introduction

Currently, calculations performed with numerical models are finding more and more applications within industrial practice, the results of such numerical simulations allowing the identification of the existing technological problem. The effect is an improvement in the production and the quality of the products. Problems as regards the modelling of the temperature field distribution within the process of cast strand solidification has been analysed by many authors. Both commercial software and original formulations have been applied [1-15].

One of the crucial parameters in the steel continuous casting process is the thickness of the shell when leaving the mould. In order to correctly determine the shell increase in the primary cooling zone, it is necessary to properly describe the solidification process of cast strand on its whole length. Note that while describing the heat transfer between the strand and the mould is a complex task, all three mechanisms of heat transfer occur within this process, these being conduction, radiation and convection [1].

This paper presents an analysis of models describing the heat transfer in the primary cooling zone of a continuous casting machine. The numerical calculation results, have been verified with industrial tests and models provided by the machine manufacturer. The impact of boundary conditions when determining the solidifying strand temperature field and the continuous casting process parameters – i.e. the length of the liquid core and the shell thickness within the primary cooling zone – was ascertained in the study.

2. The numerical model of the continuous steel casting process

Based on the technical design of the continuous casting machine operating at the Cracow Branch of ArcelorMittal, a mould with a height of 900 mm and a wall thickness of 40 mm, was designed within the model. Filling the mould with liquid steel was assumed to be at a constant level of 850 mm. At the stage of strand shape designing, the technological division into spray zones comprising the secondary cooling zone was taken into account.

2.1. Material-related parameters

The properties of the S235 steel obtained from the experimental research, and those that were calculated with the CompuTherm LLC thermodynamic databases, were used in the numerical model of the continuous process of steel casting. This model uses the enthalpy method as regards the calculations of the temperature distribution. This method is described

* AGH UNIVERSITY OF SCIENCE AND TECHNOLOGY, FACULTY OF METALS ENGINEERING AND INDUSTRIAL COMPUTER SCIENCE, AL. A. MICKIEWICZA 30, 30-059 KRAKÓW, POLAND

240

as in the equation [16].

$$H(T) = \int_0^T c_p(T)\,dt + L(1-f_s) \qquad (1)$$

The values of specific heat, and heat of solidification – as reported from the tests performed with a Netzsch STA 449 F3 Jupiter device – were implemented in the formulated numerical model [14]. Fig. 1 presents the values of specific heat as a function of temperature. Those values were utilised for further calculations.
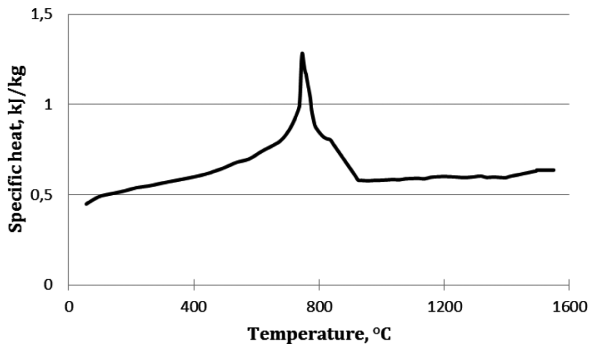

Fig. 1. Specific heat versus temperature for the S235 steel [14]

The liquidus and the solidus temperatures – along with heat conductivity, density and viscosity – were calculated with the thermodynamic databases provided, along with the Pro-CAST software. Thermal conductivity, density and viscosity were determined as a function of temperature [17].

2.2. Boundary and initial conditions

Describing the heat transfer model in the continuous steel casting process is a complex task, as all three mechanisms of heat transfer occur within this process. In the calculations presented, the heat transfer model was applied in which the temperature field could be determined by solving the Fourier equation [13]:

$$\frac{\partial(\rho c_p T)}{\partial t} = \frac{\partial}{\partial x}(\lambda \frac{\partial T}{\partial x}) + \frac{\partial}{\partial y}(\lambda \frac{\partial T}{\partial y}) + \frac{\partial}{\partial z}(\lambda \frac{\partial T}{\partial z}) + Q \qquad (2)$$

The solution to the thermal problem is the T vector, which represents the temperature values in the individual nodes of the finite element mesh. In the formulated numerical model of the continuous steel casting process, these boundary conditions may be declared in three various ways. The equation below describes the second- (the Neumann condition) and the third-type boundary conditions:

$$Q = Flux + h(T - T_a) + \sigma\varepsilon\left(T^4 - T_a^4\right) \qquad (3)$$

The heat flux may be defined directly – as the Flux value (the Neumann condition) – as well as with the convection (h – substitute heat-transfer coefficient) and radiation model (ε – emissivity). In each case – when defining the boundary conditions – the ambient temperature T_a should be indicated. The surfaces for which boundary conditions were introduced were broken down into four groups:

1. The contact of the solidifying strand surface with the inner side of the mould

2. The outer side of the mould
3. The surface of the liquid steel meniscus
4. The secondary cooling zone

For the outer side of the mould, the value of the heat transfer coefficient of 24000 W/m²K was calculated, which corresponded to the value of the heat received by the water flowing within the mould channels. This value was implemented in the 3D model of the solidifying strand created in the *Pro-CAST* environment. For the secondary cooling zone, based on the numerical values of the water flux density, a set of heat transfer coefficients was calculated for each of the spray zones. Dependence 4 was used to determine the heat transfer coefficient for each of the spray zones [13]:

$$\alpha_{spray} = 10v + (107 + 0,688v)\,w \qquad (4)$$

The values of the heat transfer coefficient within the secondary cooling zone were correlated with a strand withdrawal speed of 1m/min.

3. Variants of Calculations

The heat transfer area in the mould may be divided into three zones. These are the zone of direct contact of the liquid steel with the mould walls; the intermediary zone where a layer of solidified steel appears; and the zone with the developing air gap. The impact of functions describing the heat transfer coefficient between the strand and the mould was examined.

TABLE 1

Heat transfer coefficient in the primary cooling zone

No.	Average or maximum value	Reference:
Group I – the average HTC value on the whole length of the mould		
1	h = 1200 W/(m²K)	[2], [3]
2	h = 1300 W/(m²K)	[4]
3	h = 1500 W/(m²K)	[5], [6]
Group II – two values of heat transfer coefficients		
4	h_1 = 1163 W/(m²K) for z ⩽ 0.6m h_2 = 1395.6 W/(m²K) for z >0.6m	[7], [8]
Group III – linear variable		
5	h = 2000 - 800 W/(m²K)	[9]
6	h = 1500 - 600 W/(m²K)	[9]
Group IV – variable (various heat transfer mechanisms)		
7	h_{max} = 1300 W/(m²K)	[10]
8	h_{max} = 2500 W/(m²K)	[11]
9	h_{max} = 2000 W/(m²K)	[12]
10	h_{max} = 1300 W/(m²K)	[13]
11	h_{max} = 3097 W/(m²K)	[15]
12	h_{max} = 1600 W/(m²K)	[18,19]

Twelve models were selected for the analysis, and these were classified into four groups. The continuous casting process model described in section 2 was used for conducting the numerical calculations. Table 1 presents models, along with the literature references and the HTC values.

First, three average values of the heat transfer coefficient were calculated. Next, the model that took the step change in the value of heat transfer coefficient into account was examined. Two models were also analysed where the heat transfer coefficient changed in a linear manner. The biggest group comprises complex models that allowed the temperature distribution to be calculated with the heat transfer coefficient as a function of the strand surface temperature. Fig. 2 presents the values of the heat transfer coefficient as a function of strand surface temperature.
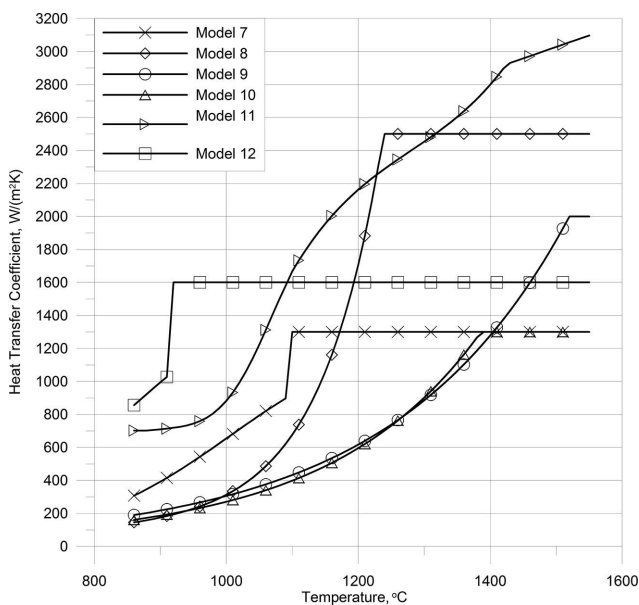
$$h = \frac{1}{R_{sk}} \quad (5)$$

where:

$$R_{sk} = R_{air} + R_{slag} \quad (6)$$

$$\frac{1}{R_{air}} = \frac{1}{R_{cond}^{air}} + \frac{1}{R_{rad}^{air}} \quad (7)$$

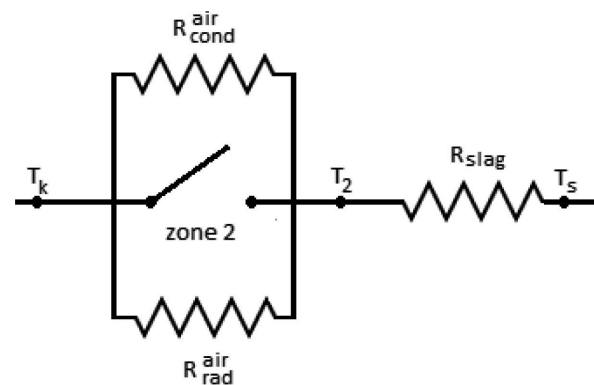$$R_{slag} = \frac{d_{slag}}{\lambda_{slag}} \quad (8)$$

Fig. 3. Diagram of thermal resistances in model 12

Fig. 2. Models of heat transfer coefficient versus temperature on the strand surface

However, the values of the heat transfer coefficients within the model were subject to verification. The limit value of the heat transfer coefficient was the criterion that allowed determining whether the assumed heat transfer coefficient in the mould-strand system was correct. It was obtained from the energy balance in the primary cooling system, which was based on the results of measurements of the increase in temperature and the volumetric flow rate of the cooling water in the continuous casting machine mould.

4. Calculation results

For the models discussed in section 3, numerical calculations of the temperature distribution in the primary and secondary cooling zones were performed. Verification was made as regards the thickness of the shell leaving the mould, the temperature of the strand surface under the mould, and the liquid core length. The liquid core length and the length of the shell leaving the mould – calculated with the numerical model of the continuous steel casting process – were compared with the models obtained from the machine manufacturer. To accomplish full verification of the temperature distribution in the primary cooling zone, the calculated heat flux rate values were read for the mould walls, and were confronted with the value of the heat flux rate as calculated on the basis of the flow rate and the difference in cooling water temperature (Table 2).

The models presented in Table 1 (except for the models with the average value of the heat transfer coefficient), define the heat transfer coefficient as a function of strand surface temperature. In order to calculate the values for model 12, the heat transfer area in the mould was divided into two zones. In the first zone, no gaseous gap was assumed and the whole space between the strand and the mould was filled with mould powder. To simplify the model it was assumed that the gap was not divided between solidified and liquid slag. The size of the area filled with the mould powder was determined on the basis of average values of powder consumption in the process of steel continuous casting. As a result of metal contraction, a gaseous gap develops at a certain distance from the meniscus: this gap separates the mould powder layer from the mould surface, additionally insulating the strand. Figure 3 presents a diagram of thermal resistances in formulated model 11.

In the model of the heat transfer in the gaseous gap, two basic heat transfer mechanisms – by radiation and by conductivity [14] – were assumed. The heat transfer coefficient between the strand surface and the mould h is:

Flux rates and temperature differences of cooling water flowing through the mould

		Average	Max
Water flow rate through mould, dm^3/min	fixed wall	2951.6	3003.9
	loose wall	2984.1	3046.9
	narrow left wall	393.5	406.3
	narrow right wall	396.9	409.4
Temperature difference,°C	fixed wall	3.7	5.0
	loose wall	3.8	5.1
	narrow left wall	4.6	6.5
	narrow right wall	4.6	6.0

Table 3 presents the shell thickness immediately under the mould, along with the value of strand surface temperature.

Comparison of the shell thickness and temperature for those selected models of heat transfer coefficient

Model	Thickness of the shell after leaving the mould, cm	Temperature °C
1	2	836
2	2.3	812
3	2.75	772
4	2.27	833
5	2.38	900
6	1.94	956
7	1.98	976
8	1.92	1050
9	1.86	1090
10	1.82	1099
11	2.51	874
12	2.52	938

For the thickness of the shell leaving the mould, the lowest value was calculated for model 10 [13] which was 1.82 cm while the strand surface temperature was 1099°C. As regards the highest shell thickness, this was calculated with the heat transfer coefficient value developed in model 3 [5,6] at the strand surface temperature of 772°C. The maximum difference in temperature, when measured at the surface of the strand leaving the mould for all models, was 327°C. The foregoing value shows a discrepancy that may occur when various models of heat transfer in the primary cooling zone – as known in literature – are applied. For all models, the length of liquid core was measured and was found to be comparable, ranging from 16.6 to 17 m. For model 11 – as developed by the authors – the shell of a thickness of 2.51 cm was obtained. The temperature at two measurement points was also checked, at the strand surface temperature of 874°C. The first measurement point was placed at a distance of about 2.5 m under the mould. For this point, the temperature values that were calculated with the numerical model were compared to those values measured

with pyrometers during the original industrial tests. Similarly, for the second measurement point (about 18 m after leaving the secondary cooling chamber), the values calculated of the strand surface temperature were compared to the temperature values recorded by a pyrometer which was permanently installed at the Cracow Branch of ArcelorMittal, Poland. The values of the strand surface temperature – when calculated with the numerical model of the continuous casting process, along with the values measured with the optical pyrometer – are presented in Table 4.

The values of the strand surface temperature calculated and measured at the reference points

	The average measured temperature °C	The calculated temperature °C
I measurement point	855	861
II measurement point	905	912

For model 11, which was formulated by the authors, an excellent level of compliance of the strand surface temperature values – calculated with the numerical model of the continuous casting process, along with the values of temperature measured during the tests conducted – was obtained. Fig. 4 presents the values of the strand surface temperature in the mould as calculated for the twelve models analysed. The temperature distribution for all models analysed is correct: however, significant differences in temperature values can be observed. The highest surface temperature along the whole length was obtained for model 10, and the lowest for model 3.
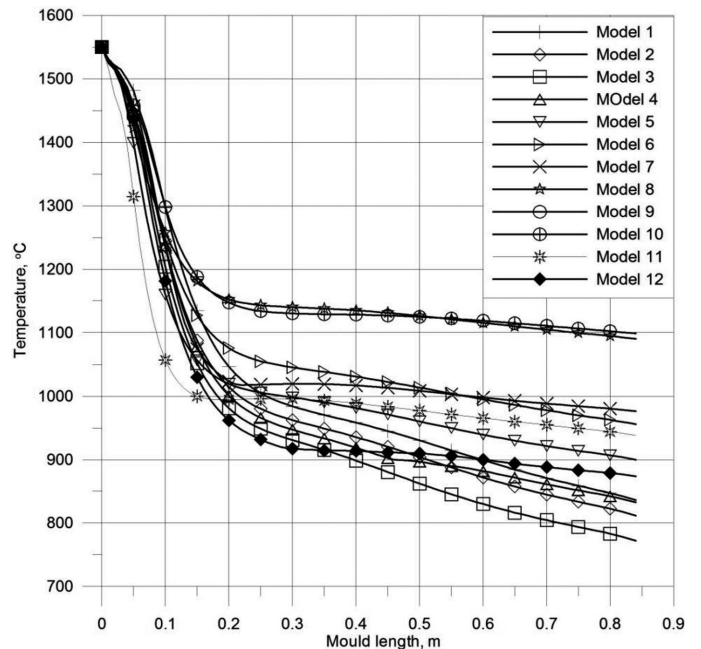

Fig. 4. The temperature distribution along the mould length

Such a significant discrepancy of the results obtained were caused by adopting various models of heat transfer in the primary cooling area, resulting in various heat fluxes transferred between the strand surface and the mould. The results obtained of temperature distribution are well correlated with the distribution of heat transfer coefficient that was assumed

for calculations for the individual models (Table 1 and Fig. 2). The adoption of an incorrect heat transfer model may result in obtaining inaccurate results of numerical calculations as regards temperatures and shell thicknesses. Analysis of the applied results obtained from these calculations indicates that the models that do not take the geometry and the arrangement of the gap between the strand and the mould into account, but adopt the average value of the heat transfer coefficient instead, may be used for preliminary process analysis.

In order to obtain a complete description of the heat exchange, complex models with a variable heat transfer coefficient on the length have to be applied, as is the case in the actual continuous casting process. Empirical models, such as, for instance, Model 11, have a narrow scope of application, being limited to the device that was used for the tests. Model 11 was formulated for cast slabs with dimensions of 1650×250 mm, along with a mould with a length of 800 mm and two casting speeds: 1.4 and 2.0 m/min.

5. Summary and conclusions

The formulated numerical model of the continuous casting of steel, as based on the input parameters calculated on the basis of industrial data, allows calculation of a reliable strand temperature distribution in the process of the continuous casting of steel. The influence of any changes in the coefficient of heat transfer between the strand and the mould were examined by calculating the temperature distribution in the primary and secondary cooling zone. Eleven referenced models were analysed, taking into account the heat transfer coefficient as a function of strand surface temperature. In addition, a proprietary heat transfer model within the primary cooling zone was formulated (model 12). We must emphasize that the maximum difference in temperature measured at the surface of the strand leaving the mould for various models was 327°C, and that the maximum difference in the thickness of the shell leaving the mould was 0.93 cm. Due to such a high discrepancy in the results, it is necessary to conduct their verification on the basis of actual data, i.e. the thermal balance and the monitoring of the strand surface temperature under the mould, which constitute the basis for determining boundary conditions in numerical models. Such detailed verification is possible for a complex model when taking into account the continuous steel casting process specificity.

Nomenclature

c_p – specific heat (kJkg^{-1}K^{-1})

d_{slag} – slag thickness (m)

$Flux$ – heat flux (W m^{-2})

f_s – solid phase fraction

h – heat transfer coefficient in the mould (W m^{-2}K^{-1})

H – enthalpy (kJ kg^{-1})

L – latent heat (kJkg^{-1})

R_{air} – heat resistance of the air gap in the mould (m^{2}K W^{-1})

R_{slag} – heat resistance of the mould powder (m^{2}K W^{-1})

R_{cond}^{air} – conduction thermal resistance in the mould (m^{2}K W^{-1})

R_{rad}^{air} – radiation thermal resistance in the mould (m^{2}K W^{-1})

t – time (s)

T – temperature (K)

T_a – ambient temperature (K)

Q – the heat source term (W m^{-3})

v – water drops' velocity (m s^{-1})

w – water flux density (dm^{3}m^{-2} s^{-1})

x, y, z – the 3D coordinate axes

α_{spray} – heat transfer coefficient for individual spray zone (W m^{-2}K^{-1})

ρ – density (kg m^{-1})

σ – Stefan-Bolzmann constant (W m^{-2}K^{-4})

ε – emissivity

λ – thermal conductivity (W m^{-1}K^{-1})

λ_{slag} – coefficient of heat transfer through the slag (W m^{-1}K^{-1})

REFERENCES

[1] T. Telejko, Z. Malinowski, M. Rywotycki, Archives of Metallurgy and Materials **54**, 837-844 (2009).

[2] M. Biedrońska, R Grzymkowski, Krzepnięcie Metali i Stopów **19**, 11-19 (1994).

[3] M. Biedrońska, R. Grzymkowski, Krzepnięcie Metali i Stopów **18**, 21-28 (1993).

[4] A. Kapusta, A. Wawrzynek, Krzepnięcie Metali i Stopów **18**, 87-94 (1993).

[5] A. Kapusta, A. Wawrzynek, Krzepnięcie Metali i Stopów **16**, 150-158 (1987).

[6] S.H. Seyedein, M. Hasan, Int. J. Heat Mass Transfer **40**, 18, 4405-4423 (1997).

[7] X.K. Lan, J.M. Khodadadi, International Journal of Heat and Mass Transfer. **44**, 953-965 (2001).

[8] X.K. Lan, J.M. Khodadadi, International Journal of Heat and Mass Transfer **44**, 3431-3442 (2001).

[9] R.B. Mahaparta, J.K. Brimacombe, I.V. Samarasekera, Metallurgical and Materials Transactions B **22B**, 6, 875-888 (1991).

[10] J. Falkus, K. Miłkowska-Piszczek, M. Rywotycki, E. Wielgosz, Journal of Achievements in Materials and Manufacturing Engineering **55**, 2, 668-672 (2012).

[11] J.K. Park, B.G. Thomas, I.V. Samarasekera, Ironmaking and Steelmaking **29**, 5, 359-375 (2002).

[12] Z. Malinowski, T. Telejko, B. Hadała, Archives of Metallurgy and Materials **57**, 1, 325-331 (2012).

[13] M. Rywotycki, K. Miłkowska-Piszczek, L. Trebacz, Archives of Metallurgy and Materials **57**, 1, 385-393 (2012).

244

[14] A. Buczek, A. Burbelko, P. Drożdż, M. Dziarmagows-
ki, J. Falkus, M. Karbowniczek, Tomasz Kargul,
K. Miłkowska-Piszczek, M. Rywotycki, K. Sołek, W.
Ślęzak, T. Telejko, L. Trębacz, E. Wielgosz, Modelowanie
procesu ciągłego odlewania stali – monografia, Radom 2012.

[15] J.S. Ha, J.R. Cho, B.Y. Lee, M.Y. Ha, Journal of Material
processing Technology **113**, 1-3, 257-261 (2001).

[16] ProCAST 2013, User Manual.

[17] K. Miłkowska-Piszczek, M. Korolczuk-Hejnak, Archives of
Metallurgy and Materials **58**, 4, 1267-1274 (2013).

[18] K. Miłkowska-Piszczek, PhD Thesis: Opracowanie i zas-
tosowanie numerycznego modelu procesu COS do wyznaczenia
technologicznych parametrów odlewania stali S235, AGH Uni-
versity of Science and Technology, Kraków, 2013.

[19] K. Miłkowska-Piszczek, J. Falkus, Metalurgija **53**, 4, 571-573
(2014).